Carbohydrate Polymers 80 (2010) 387–393

Contents lists available at ScienceDirect

Carbohydrate Polymers

journal homepage: www.elsevier.com/locate/carbpol

Rapid crystallization of poly(3-hydroxybutyrate-co-3-hydroxyhexanoate) copolymer accelerated by cyclodextrin-complex as nucleating agent

Tungalag Dong [a], Takafumi Mori [a], Taizo Aoyama [b], Yoshio Inoue [a,*]

[a] Department of Biomolecular Engineering, Tokyo Institute of Technology, Nagatsuta 4259-B55, Midori-ku, Yokohama 226-8501, Japan
[b] Polymers Processing R&D Group High Performance, Polymers Division, Kaneka Corporation, 5-1-1 Torikai-Nishi Settsu Osaka, Japan

ARTICLE INFO

Article history:
Received 9 July 2009
Received in revised form 9 November 2009
Accepted 19 November 2009
Available online 24 November 2009

Keywords:
Biodegradable polymer
Poly(3-hydroxybutyrate-co-3-hydroxyhexanoate)
Cyclodextrin
Crystallization
Nucleation

ABSTRACT

The nucleation effect of inclusion complex (IC) between poly(3-hydroxybutyrate) (PHB) and alpha-cyclodextrin (α-CD) on the rapid crystallization of a series of bacterial copolyesters poly(3-hydroxybutyrate-co-3-hydroxyhexanoate) (PHBH) with 3HH molar fraction ranging from 7 to 18 mol% was investigated by differential scanning calorimetry (DSC) and a polarized optical microscopy (POM). The results were compared with the effectiveness of PHB particles as a nucleation agent. Both the PHB-IC and the PHB particles enhance the nucleation and crystallization of PHBH, whereas the PHB-IC particles show much more effective nucleation ability than the PHB particles for the crystallization of PHBH. With introduction of PHB-IC, PHBH with 18% 3HH unit can finish crystallization during cooling process from the melt at 10 °C/min, and its crystallinity is greatly increased. The crystallization half-time ($t_{1/2}$) of PHBH with 7–18% 3HH units decreases significantly in the presence of PHB-IC. The PHB crystals in the PHB-IC are suggested to favorably nucleate PHBH crystallization with the same crystalline lattice.

1. Introduction

Bacterially synthesized poly(hydroxyalkanoate)s including poly(3-hydroxybutyrate) (PHB) homopolymer and related copolymers is a naturally occurring thermoplastic which has attracted the attention of industry and researchers for its special properties of environmental biodegradability and biocompatibility (Sudesh, Abe, & Doi, 2000). PHB is a completely biodegradable, highly hydrophobic thermoplastic polyester material (Sudesh et al., 2000; Verhoogt, Ramsay, & Favis, 1994). The chemical structure and physical properties of PHB are very similar to those of certain petroleum-based synthetic polymers. Therefore, PHB has been the subject of extensive studies as an environmentally friendly polymeric material (He, Zhu, & Inoue, 2004; Misra, Valappil, Roy, & Boccaccini, 2006; Verhoogt et al., 1994). However, PHB has several inherent deficiencies as an engineering material, including its brittleness and thermal instability above its melting point (Barham & Keller, 1986). These problems have been the major bottlenecks for its large-scale commercial applications.

For the purpose of industrial applications, 3-hydroxybutyrate (3HB) copolymer with 3-hydroxyhexanoate (3HH), that is, poly(3-hydroxybutyrate-co-3-hydroxyhexanoate) (PHBH), was introduced to enhance the processability and mechanical properties of PHB. The 3HH unit with medium-length side groups was incorporated into the molecular chain of PHB to attain more desirable properties (Asrar et al., 2002; Cheng, Lin, Su, Chen, & Sun, 2008; Doi, Kitamura, & Abe, 1995; Feng, Yoshie, Asakawa, & Inoue, 2004). It was reported that the crystallinity of PHBH decreases from 60% to 18% as the 3HH fraction increases from 0 to 25 mol%, and the PHBH becomes soft and flexible with an increase in the 3HH fraction. The melting temperature of PHBH decreases steeply with the increase of 3HH molar fraction. Contrast to conventional brittle PHB, the mechanical properties of PHBH is comparable to those of high-density polyethylene and polypropylene in strength, flexibility and toughness. Furthermore, the PHBH exhibits some other attractive properties, e.g., anaerobic and aerobic biodegradability, hot alkaline digestibility, hydrolytic stability, good odor and oxygen barrier capability, and excellent surface properties for printing.

The PHBH is produced by a fermentation process to produce extremely pure material after solvent extraction from bacterial cells, resulting in an unusually low nucleation density. Furthermore, as the 3HH units are excluded from the PHB crystalline lattice during the crystallization of PHBH with relatively high HB unit content, they significantly hinder the crystallization of the HB units (Doi et al., 1995; Sato et al., 2004). Therefore, the PHBH materials show the much slower crystallization rate and lower crystallinity, which becomes more serious as the 3HH unit content increases. This poor processability is one of the major drawbacks of the PHBH-related materials.

As is well known, an addition of appropriate nucleation agents can help to increase the nucleation density and promote the crys-

* Corresponding author. Tel.: +81 45 924 5794; fax: +81 45 924 5827.
E-mail address: inoue.y.af@m.titech.ac.jp (Y. Inoue).

0144-8617/$ - see front matter © 2009 Elsevier Ltd. All rights reserved.
doi:10.1016/j.carbpol.2009.11.036

tallization of polymers, and thus it is expected to inhibit the embrittlement and improve the processing efficiency of polymeric materials. However, there are few reports on rapid crystallization of PHBH with introduction of nucleating agent. Luo et al. reported the effect of L-Phenylalanine (L-Phe) on the crystallization of PHBH with 13.5 mol% of 3HH unit, they found that 1wt% of L-Phe shortens the crystallization half-time of PHBH (Luo, Xu, & Chen, 2008). Tajima et al. investigated the nucleation effects of boron nitride (BN) and PHB on the crystallization of PHBH with 21 mol% 3HH units (Tajima, Dong, Hirose, Aoyama, & Inoue, 2008). Interestingly, both BN and PHB particles cannot show any nucleation effect for crystallization of PHBH, while the PHBH/PHB/BN ternary blend shows faster crystallization. Most effective nucleating agent for PHBH has been found by Pan et al. recently (Pan, Liang, Nakamura, Miyagawa, & Inoue, 2009). They used uracil as the nucleating agent for PHBH with 3HH content of 5, 10, 18 mol%. The crystallization rate of PHBH is greatly enhanced and the nucleation density is increased by several orders of magnitude by an addition of small amounts of uracil.

The cyclodextrins (CDs) comprise a family of cyclic oligosaccharides, and several members of this family are used industrially in pharmaceutical and related applications (Szejtli, 1998; Wenz, 1994). These biocompatible cyclic oligosaccharides do not elicit immune responses and have low toxicities in animals and humans. α-CD, β-CD, and γ-CD are typical CDs consisting of 6, 7 and 8 glucopyranose units linked by α-1,4-glycosidic bonds, respectively. Since Harada et al. have found that α-CD forms inclusion complex (IC) with linear polymer (Harada & Kamach, 1990), the CD-ICs with polymers have attracted much attention due to their unique supramolecular architectures, such as polyrotaxane and hydrogel, as well as good models for macromolecular recognition in biological systems (Huang & Gibson, 2005; Li et al., 2006; Loethen, Kim, & Thompson, 2007; Okumura & Ito, 2001; Ooya & Yui, 1999; Wenz, Han, & Müller, 2006). Tonelli et al. found that coalescence of guest polymers from their ICs with CDs can result in a significant improvement of their physical property caused by modification of the structure, morphology, and even conformation that are observed for their coalesced bulk samples (Rusa et al., 2004; Shuai, Porbeni, Wei, Bullions, & Tonelli, 2002; Wei, Shuai, & Tonelli, 2003; Wei et al., 2002).

Recently we have reported that α-CD greatly enhance the crystallization of biodegradable semicrystalline polymers, such as PHB, poly(ε-caprolactone), poly(ethylene glycol), poly(butylene succinate) and poly(butylene adipate) (Dong, Kai, & Inoue, 2007b; Dong, Kai, Pan, Cao, & Inoue, 2007a; Dong et al., 2009; He & Inoue, 2003). It is concluded that IC of a given polymer could greatly enhance the nucleation and crystallization of the polymer itself. In the other word, the exterior parts of polymer segment included in the α-CD cavities are favorable to induce crystallization of bulk polymer with the same crystalline lattice. Doi et al. (1995) have reported that 3HH units are excluded from the PHB crystalline phase, and only one crystalline phase of PHB lattice is observed for the PHBH copolymers with 3HH unit compositions of up to 25 mol%. Thus, it is expected that the IC of PHB with α-CD (PHB-IC) should enhance the crystallization of PHBH, because PHB-IC greatly accelerates the PHB crystallization.

As the CDs are natural products and they are safe and environment friendly (Davis & Brewster, 2004), and furthermore their nucleation ability on the crystallization of aliphatic polyesters is comparable to those of conventional nucleation agents, the CDs are expected to be ideal candidates as the green nucleation agents for the crystallization of biodegradable polymers. In this study, the effect of PHB-IC on the nucleation and crystallization of PHBH will be investigated by the differential scanning calorimetry (DSC) and polarized optical microscopy (POM). The nucleation effectiveness of PHB-IC will be compared to that of PHB particles.

2. Experimental

2.1. Materials

A series of bacterial PHBH samples with 3HH molar fractions 7, 12, and 18 mol%, respectively, were kindly supplied by Kaneka Corporation, Osaka, Japan. The samples coded as PHBH7, PHBH12, and PHBH18, where the numerals denote the molar fractions of the 3HH unit. The number average molecular weights (M_n) of PHBH7, PHBH12, and PHBH18 are 9.0×10^4, 9.2×10^4, and 1.1×10^5, and their polydispersity indexes (M_w/M_n) are 2.6, 2.6, and 3.3, respectively. α-CD was purchased from NACALAI TESQUE, INC. Kyoto, Japan and was dried in vacuum at 90 °C for 8 h before use.

PHB sample was purchased from PHB Industrial S. A., Brazil. The low-molecular-weight PHB sample (M_w = 5,700, M_w/M_n = 1.9) was obtained by hydrolysis of high-molecular-weight PHB ($M_n = 7.8 \times 10^4$, M_w/M_n = 3.5) (Iwata, Doi, Kasuya, & Inoue, 1997). Briefly, 3 g of PHB was dissolved in 300 mL of chloroform, after adding 120 mL of 2 N aqueous KOH and 4 mg of 18-crown-6 ether to the PHB solution, then the mixture was stirred at 25 °C for 24 h. Finally, the organic layer was precipitated into methanol. Before use, the polymer samples were purified by precipitation into ethanol from chloroform solution and then were dried at 40 °C under vacuum for 1 week.

2.2. Preparation of IC sample

For the preparation of PHB-IC, both the solutions of PHB (low molecular weight, 0.2 g) in dimethyl sulfoxide (DMSO; 2 mL) and α-CD (1.0 g) in DMSO (2 mL) were heated to 80 °C in order to obtain the clear solutions. Subsequently, both solutions were mixed together and stirred at 80 °C for 3 h, and then the mixture was further stirred at 30 °C for 24 h. Upon adding excess amount of chloroform (50 mL) into the mixture, the solution immediately became turbid. The precipitated products were filtrated and then washed by chloroform to remove the free PHB. The remained powder was dried under a vacuum at 40 °C for 24 h, then washed with water to remove the free α-CD, and again dried under the vacuum at 40 °C for further 1 week.

2.3. Sample preparation

The PHB powder, α-CD particles and PHB-IC were used as the nucleating agents for crystallization of PHBH samples. The 2 wt.% of nucleating agent was dispersed in acetone, and then the suspension was treated by ultrasonic treatment (BRANSON-B3200 water bath, at 47 kHz and 120 W) at 25 °C fro 5 min. Finally, PHBH (0.1 g/mL) was added into the suspension, and the solvent was allowed to evaporate during rigorous stirring. The resultant films were dried at 25 °C under vacuum for 1 week before analysis. It is noted that the PHBH is soluble in acetone, whereas the PHB, α-CD and PHB-IC are insoluble in acetone.

2.4. The wide-angle X-ray diffraction (WAXD)

The WAXD pattern of the sample was recorded on a Rigaku RU-200 (Rigaku Corp. Tokyo, Japan) using Nickel-filtered Cu-K_α radiation (40KV, 200 mA) with the 2θ value ranging from 10° to 35° at a scanning rate of 1°/min.

2.5. Host–guest stoichiometry of PHB-IC

The host–guest stoichiometry of PHB-IC was estimated by solution ^{1}H NMR spectra recorded on a Bruker Ultrashield 600 MHz/54 mm NMR spectrometer in DMSO-d_6 at 80 °C.

2.6. Differential scanning calorimetry (DSC)

The DSC thermograms of the sample (about 8 mg) pre-sealed into an aluminum pan was recorded on a Pyris Diamond DSC instrument (PerkinElmer Japan Co., Ltd. Yokohama, Japan). In the non-isothermal crystallization, the sample was heated to 180 °C and held for 2 min, and then cooled at a rate of 10 °C/min to induce the non-isothermal crystallization. In the isothermal crystallization, after heated to 180 °C and held for 2 min, the sample was quenched to the desired crystallization temperature.

2.7. Polarized optical microscopy (POM)

The POM was performed on an Olympus BX90 POM (Olympus Corporation, Tokyo, Japan) equipped with a digital camera. The polymer sample was placed between a slide glass and a cover slip and was heated on a Mettler FP82HT hot stage. The samples (about 0.2 mg) were first heated to 180 °C and held for 2 min, then quenched to the desired crystallization temperature.

3. Results and discussion

3.1. Characterization of PHB-IC

The formation of PHB-IC was characterized by WAXD, ^{1}H NMR and DSC analyses. As shown in Fig. 1, the WAXD patterns strongly support the formation of inclusion complex between PHB and α-CD. Two prominent diffraction peaks at 13.4° and 16.9° are found in the diffraction pattern of crystalline PHB. However, the diffraction patterns of PHB-IC are very different from those of PHB and α-CD. A new strong diffraction peak appeared at 19.9° is present in the diffraction pattern of PHB-IC, which is well known to be the characteristics of α-CD-based IC crystals adopting the channel structure (Takeo & Kuge, 1970). This characteristic peak of channel structure ICs at 19.9° is not present in the diffraction pattern of α-CD, which adopts a cage structure (Peet, Rusa, Hunt, Tonelli, & Balik, 2005). It is notable that the characteristic peaks of PHB at 13.4° and 16.9° are also found in the WAXD pattern of PHB-IC, indicating that there is still the PHB crystalline region outside the α-CD cavity even after IC formation.

The partial coverage of each PHB chain by α-CD molecules is also demonstrated by the ^{1}H NMR spectrum of PHB-IC in DMSO-d_6. It is known that the depth of the α-CD cavity is about 7.9 Å, which is equal to the length of 1.5 3HB monomeric repeat units. From ^{1}H NMR spectrum, the molar ratio of α-CD molecule to the monomeric repeat unit of PHB is calculated to be 10.1, which is much higher than 1.5, indicating that about 85% segments of PHB are uncovered by α-CD cavities.

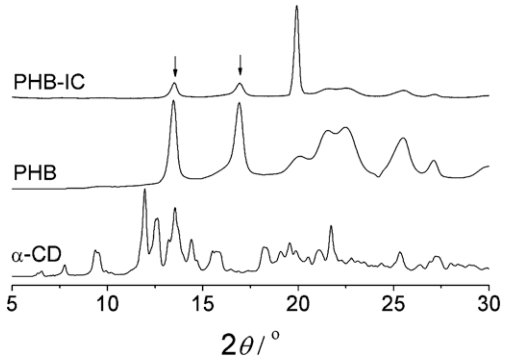

Fig. 1. WAXD patterns of α-CD, PHB and PHB-IC.

The melting behavior of α-CD, PHB and PHB-IC was investigated by DSC measurement, as shown in Fig. 2. α-CD does not show any detectable thermal transitions in the heating scan. The melting peak (T_m) of neat PHB is about 176 °C. The PHB-IC shows very small melting peak at a slightly lower temperature than that of the PHB, indicating that uncovered parts of PHB are crystallizable and the stability of crystal may be lower than that of neat PHB crystal. In the case of neat PHB, the value of melting enthalpy (ΔH_m) is calculated to be 70.8 J/g. Upon formation of IC, the value of ΔH_m of PHB is greatly decreased to only 7.7 J/g (normalized with PHB weight percent), indicating that the crystallization of PHB is remarkably suppressed in the PHB-IC.

3.2. Spherulitic morphology of PHBH

The polarized optical microscopy (POM) was used to monitor the growth and size of the spherulites. In Fig. 3 are shown the spherulitic morphologies of PHB and PHBH18 with nucleating agents. In the isothermal crystallization at 130 °C, the diameter of the PHB spherulites reaches up to 2000 μm before they impinge each other, as the amount of the nuclei is quite few in the PHB. Upon addition of PHB-IC, the average diameter of the spherulites is decreased, and the nuclear density in PHB/PHB-IC is greatly increased.

In the case of PHBH18 samples, their spherulite growth was monitored at 100 °C after quenched directly form 180 °C. The spherulite size of neat PHBH18 is very large and the nuclear density is quite low. With the addition of the PHB particles, the spherulite number increases slightly, but the α-CD particles did not show any nucleation effect on crystallization of PHBH18. However, with the incorporation of PHB-IC, the spherulite size decreases dramatically, and the spherulite number is much larger than that of neat PHBH18 crystallized under the same conditions. Obviously, the PHB-IC acts as a good nucleating agent for the PHB and PHBH18 crystallization.

3.3. Non-isothermal crystallization of PHBH

The effects of PHB, α-CD, and PHB-IC on the crystallization of PHBH18 were compared by DSC measurements. Fig. 4 shows the DSC curves of non-isothermal crystallization and subsequent melting scans for neat and nucleated PHBH18, respectively. The crystallization temperature (T_c), crystallization enthalpy (ΔH_c), cold-crystallization temperature (ΔH_{cc}), T_m and ΔH_m are summarized in Table 1.

In Fig. 4(A), the DSC cooling curves observed at cooling rate of 10 °C/min reveal the relative nucleation abilities of PHB, α-CD and PHB-IC, as indicated by the peak crystallization temperature T_c and the temperature range over which the polymer samples crystallized. Usually, a high T_c and a narrow crystallization temper-

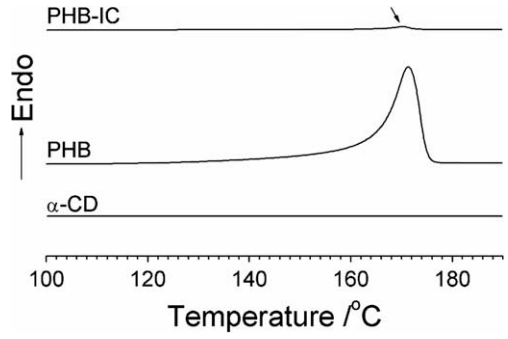

Fig. 2. DSC melting exotherms of α-CD, PHB and PHB-IC during heating scan at rate of 10 °C/min.

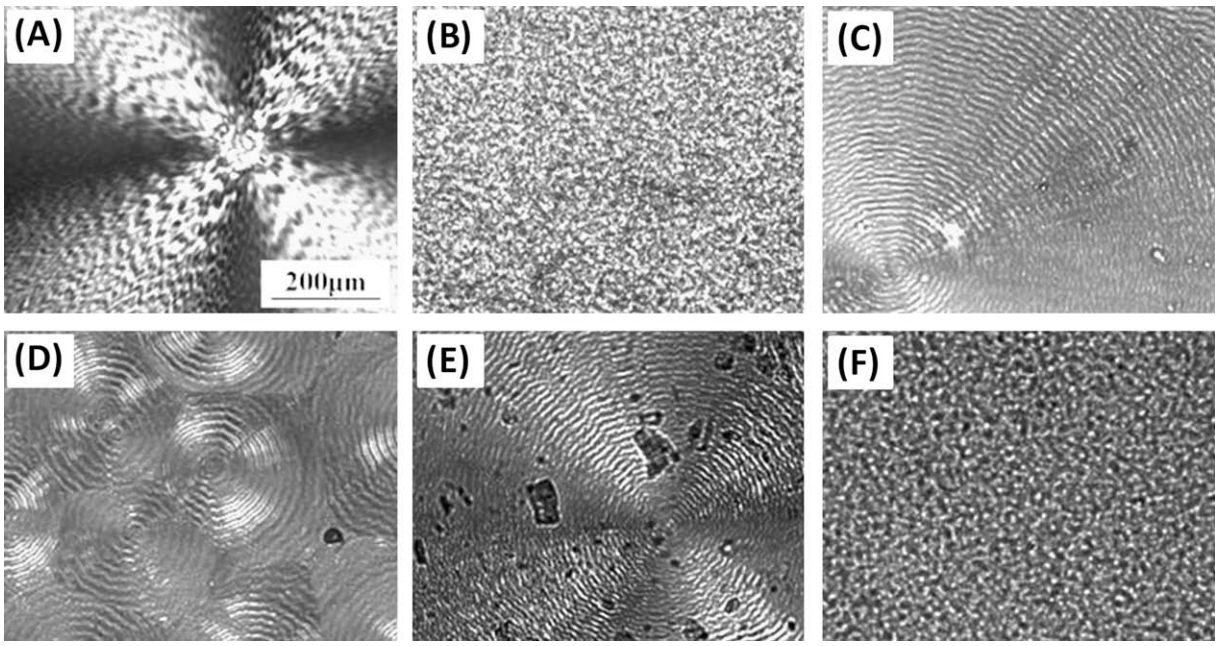

Fig. 3. POM images of PHB, PHBH18 and their blends with nucleating agents: (A) Neat PHB; (B) PHB/PHB-IC; (C) Neat PHBH18; (D) PHBH18/PHB; (E) PHBH18/α-CD and (F) PHBH18/PHB-IC.

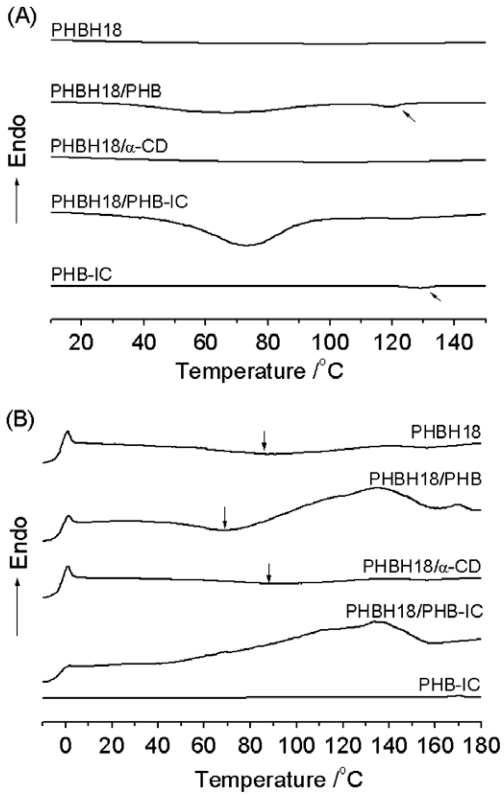

Fig. 4. DSC curves of (A) non-isothermal crystallization and (B) subsequent heating scans for PHB-IC, neat PHBH18 and its blends with nucleating agents. Both the cooling and heating rates are 10 °C/min.

ature range indicate faster crystallization. The crystallization rate of the neat PHBH is very slow. Upon cooling at 10 °C/min, the crystallization peak is not detected, and a cold-crystallization peak appears at the temperature range of 60–110 °C in the subsequent heating process, as shown in Fig. 4(B).

With the addition of PHB, the PHBH18/PHB sample shows two crystallization peaks. The small peak appeared at 119 °C is corresponding to crystallization of PHB, while the broad peak at range of 20–100 °C is corresponding to crystallization of PHBH18. In its subsequent heating curves, the T_{cc} value of PHBH18 shifts to lower temperature. Although the crystallization of PHBH is accelerated by the incorporation of PHB particles, the PHBH18/PHB sample cannot complete the crystallization during cooling process at 10 °C/min.

Obviously, the DSC curve of the PHBH18/α-CD sample is very similar to that of the neat PHBH18, and the cold-crystallization peak of PHBH18 is not changed by an addition of α-CD. However, with the addition of PHB-IC, the crystallization peak of PHBH18 appears at a higher temperature about 73 °C and became much sharper than that of the PHBH18/PHB sample. The cold-crystallization peak of PHBH18/PHB-IC can not be detected in its subsequent heating scan. Furthermore, the crystallinity of PHBH increased from 0.1% to 23.4%. It can be concluded that the PHB-IC accelerates the crystallization of PHBH18 significantly, and its nucleation effect is much greater than that of PHB and α-CD particles.

3.4. Isothermal crystallization behavior of PHBH

The isothermal crystallization of neat and nucleated PHBH copolymers with 3HH content of 7, 12, 18 mol% at different T_cs were investigated by DSC. For the sake of clarity, only the DSC curves of PHBH18 samples are shown here. Fig. 5 presents the isothermal crystallization curves for the neat PHBH18 and PHBH18 containing PHB, α-CD and PHB-IC crystallized at 100 °C for 60 min.

Obviously, the crystallization rate of neat PHBH and PHBH/α-CD is extremely slower, and the crystallization of PHBH cannot complete within 60 min. With the addition of PHB and PHB-IC, the crystallization peak becomes sharp and the crystallization time shortens.

Crystallization kinetics was determined from the isothermal DSC measurements. The isothermal heat flow curve was integrated to determine the degree of crystallinity of the sample as a function of crystallization time. The relative crystallinity X_t at any given time was calculated from the integrated area of the DSC curve from

Table 1
Non-isothermal crystallization and melting behavior of PHBH18 and PHBH18 containing 2 wt.% PHB, α-CD or PHB-IC as nucleating agents.

Sample	T_c (°C)	ΔH_c (J/g)	T_{cc} (°C)	ΔH_{cc} (J/g)	T_m (°C)	ΔH_m (J/g)	X_c (%)
PHBH18	N.D.	N.D.	86	−1.9	136	2.1	0.1
PHBH18/PHB	66	−13.4	68	−6.7	136	23.8	11.7
PHBH18/α-CD	N.D.	N.D.	87	−1.2	136	1.3	0.1
PHBH18/PHB-IC	73	−31.1	N.D.	N.D.	137	34.1	23.4

'N.D.' denotes 'not detected'; the crystallinity (X_c) values of PHBH are estimated by comparing ΔH_m with the value of an infinitely large crystal of PHB (ΔH_m^0), taken as $\Delta H_m^0 = 146$ J/g($X_c = (\Delta H_m + \Delta H_{cc})/\Delta H_m^0 \times 100\%$) (Barham, Keller, Otun, & Holmes, 1984).

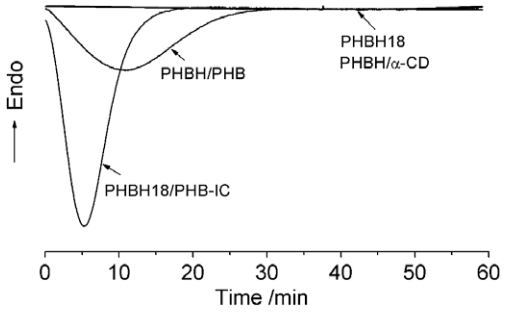

Fig. 5. DSC curves of PHBH18 and its blends with nucleating agents isothermally crystallized at 100 °C for 60 min.

time $t = 0$ to $t = t$ divided by the integrated area of the whole heat flow curve. The isothermal bulk crystallization kinetics was analyzed with the Avrami equation (Avrami, 1939, 1940, 1941):

$$X_t = 1 - \exp(-kt^n), \quad (1)$$

where n is an index related to the dimensional growth and the way of formation of primary nuclei, and k is the overall rate constant associated with both nucleation and growth contributions. The linear form of Eq. (1) is given as Eq. (2):

$$\log[-\ln(1 - X_t)] = \log k + n \log t, \quad (2)$$

n and k are obtained by plotting $\log[-\ln(1 - X_t)]$ against $\log t$. The crystallization half-time $t_{1/2}$, which is defined as the time when the crystallinity arrives at 50%, can be determined from the kinetics parameters measured by using the following equation:

$$t_{1/2} = \left(\frac{\ln 2}{k}\right)^{\frac{1}{n}} \quad (3)$$

The crystallization half-time $t_{1/2}$ of the samples was estimated by isothermal crystallization at 60, 80 and 100 °C with Avrami theory and Eq. (3). The calculated $t_{1/2}$ values are shown in Table 2. For the PHBH18 samples, the $t_{1/2}$ values of neat PHBH18 are much larger than 60 min. With the addition of the PHB particles, the $t_{1/2}$ values shorten to about 8 min. The PHB-IC is most effective on crystallization half-time, the $t_{1/2}$ values of PHBH18 further shortens to 2.6, 2.5 and 4.8 at 60, 80, and 100 °C, respectively, by addition of PHB-IC.

For the PHBH12 samples, the $t_{1/2}$ value of neat PHBH12 at 60 °C is about 30 min, while the $t_{1/2}$ value is larger than 60 min crystallized at above 80 °C, indicating that the crystallization rate of PHBH12 is very slow. The PHB particles decrease the $t_{1/2}$ value to within 7 min, while the PHB-IC further decreases the $t_{1/2}$ value to within 3 min. Similarly, both PHB and PHB-IC shortens the crystallization half-time of PHBH7, and the PHB-IC exhibits much more effective nucleation ability than PHB for PHBH7.

Table 2
The crystallization half-time $t_{1/2}$ for PHBH samples isothermally crystallized at various temperatures.

3HH unit content in PHBH (mol%)	Nucleating agent	$t_{1/2}$ (min)		
		T_c = 60 °C	T_c = 80 °C	T_c = 100 °C
18	–	>60	>60	>60
	PHB	8.2	8.1	8.1
	PHB-IC	2.6	2.5	4.8
12	–	29.7	>60	>60
	PHB	5.5	6.4	6.9
	PHB-IC	1.3	1.3	2.5
7	–	7.4	17.7	>60
	PHB	2.9	5.5	6.2
	PHB-IC	0.2	0.2	1.3

3.5. Discussion

As described above, the crystallization rates of PHBH with 3HH molar fractions 7, 12, and 18 mol% are greatly accelerated by introduction of PHB-IC. They form the common PHB homopolymer type crystals which supported by the WAXD results (data not shown here). A possible mechanism can be given to this acceleration of PHBH crystallization as below.

PHB particles also enhance slightly the PHBH crystallization. This may be attributable to that an epitaxial crystallization of PHBH occurs on the interface between PHBH and PHB domains. In Fig. 6 are shown the optical micrographs of the morphologies of PHBH18 crystallized on the PHB and PHB-IC substrates. In this case, the neat PHBH18 cooled to 150 °C just after melted at 180 °C for 2 min, and then the PHB film or the PHB-IC particles immersed into the molten sate PHBH18. Finally, the samples were quenched to 100 °C to observe the spherulite growth during the isothermal crystallization.

Over a period of time, the nucleation and spherulite growth of PHBH can be observed at the boundary region between the PHBH and the PHB substrate, while the spherulites with detectable size cannot be observed in the region away from the PHBH-PHB interface as shown in Fig. 6(A). It is concluded that the nucleation of PHBH crystal with the same crystalline lattice as the PHB crystal is favorably enhanced by the presence of the PHB crystals.

In the PHBH18/PHB sample (Fig. 4(A)), during the cooling process after melted at 180 °C, the PHB is firstly crystallized at higher

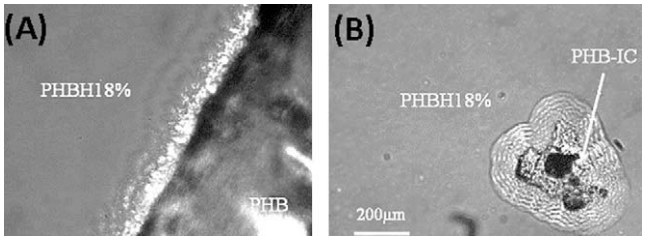

Fig. 6. POM image observed at 100 °C, showing a boundary crystalline region of PHBH18 crystallized from melt on the surface of PHB film (A) and PHB-IC particles (B).

temperature region around 119 °C, then the PHBH18 is subsequently crystallized at lower temperature range of 20–100 °C. When the increase in molten temperature to 190 °C, the exothermic peaks of both PHB and PHBH crystallization are not detected during the cooling scan at 10 °C/min (data not shown here), indicating that the PHB particles lost its nucleation capability. Because the thermal history of PHB is erased by increasing the temperature to over 188 °C (Organ & Barham, 1991), the small amount of the PHB particles is completely molted and is freely dispersed into the PHBH matrix. As PHB and PHBH with low 3HH unit content are miscible in the amorphous (molten) state (Feng et al., 2003), the decrease in nucleation effectiveness of the PHB particles is attributable to the loss of the solid PHB-molten PHBH interface, which supports the nucleation of PHBH crystallization.

Therefore, when the molten temperature is below 188 °C, the PHB particles just melted, and should maintain its original domain. Due to the remaining of thermal history, the PHB domain crystallizes quickly, and the faces of as-produced PHB crystals subsequently induce the nucleation of PHBH crystallization.

From the structural analysis of PHB-IC, the long polymer chains, the parts of which are found to be included inside the α-CD cavities, are crystallizable. As shown in Fig. 4(A), in the cooling curve of PHB-IC at 130 °C, a small exothermic peak corresponding to PHB crystallization is detected, which is higher than T_c of neat PHB. Although the crystallinity of PHB is greatly decreased upon formation of IC, the crystallization of small amount of the PHB segment uncovered by the α-CD cavities is still fast. This result may be attributable to the limited mobility of uncovered part of the PHB segments constrained by another part resided in the α-CD cavity.

Furthermore, the channel structure of α-CD in ICs is very stable even at higher temperature (Mori, Dong, Yazawa, & Inoue, 2007). As a result that the PHB chains are bundled by the α-CD molecules in the PHB-IC, the PHB chains are unable to disperse into the PHBH molten state even at high temperature. There are always the mobility-constrained but crystallizable PHB domains uncovered by the α-CD cavities. Therefore, it is suggested reasonably that the crystallization of bulk PHBH is induced by partially crystallized PHB segments on the surface of the PHB-IC particles, that is, the epitaxial crystallization occurs.

This suggestion is directly supported by the POM observation, as shown in Fig. 6(B). The dense population of spherulites grows around the PHB-IC particles in a very short time. This is a direct consequence of the increase in the density of nucleating sites of PHBH in the vicinity of PHB-IC particles. These results indicated that the IC state of PHB with α-CD is more effective for promoting the crystallization of PHBH than the free-state PHB particles.

4. Conclusion

The nucleation effect of PHB-IC on the crystallization of PHBH with 3HH unit fraction of 7–18% was investigated by DSC and POM analyses. Both the PHB-IC and the PHB particles enhance the nucleation and crystallization of PHBH, whereas PHB-IC shows much more effective nucleation ability than the PHB particles. These results indicated that the complex state of PHB with α-CD is more effective for promoting the crystallization of PHBH than the free-state PHB particles. It is concluded that the nucleation of PHBH with the same crystal lattice as PHB is favorably enhanced by the PHB crystals.

Acknowledgment

Tungalag DONG gratefully acknowledges Japan Society for the Promotion of Science for providing the fellowship and the grant-in-aid to do this research at the Tokyo Institute of Technology.

References

Asrar, J., Valentin, H. E., Berger, P. A., Tran, M., Padgette, S. R., & Garbow, J. R. (2002). Biosynthesis and properties of poly(3-hydroxybutyrate-co-3-hydroxyhexanoate) polymers. *Biomacromolecules, 3*, 1006–1012.

Avrami, M. (1939). Kinetics of phase change. I general theory. *Journal of Chemical Physics, 7*, 1103–1112.

Avrami, M. (1940). Kinetics of phase change. II transformation-time relations for random distribution of nuclei. *Journal of Chemical Physics, 8*, 212–224.

Avrami, M. (1941). Granulation, phase change, and microstructure kinetics of phase change. III. *Journal of Chemical Physics, 9*, 177–184.

Barham, P. J., & Keller, A. (1986). The relationship between microstructure and mode of fracture in polyhydroxybutyrate. *Journal of Polymer Science. Part B, Polymer Physics, 24*, 69–77.

Barham, P. J., Keller, A., Otun, E. L., & Holmes, P. A. (1984). Crystallization and morphology of a bacterial thermoplastic: Poly-3-hydroxybutyrate. *Journal of Materials Science, 19*, 2781–2794.

Cheng, M., Lin, C., Su, H., Chen, P., & Sun, Y. (2008). Processing and characterization of electrospun poly(3-hydroxybutyrate-co-3-hydroxyhexanoate) nanofibrous membranes. *Polymer, 49*, 546–553.

Davis, M. E., & Brewster, M. E. (2004). Cyclodextrin-based pharmaceutics: Past, present and future. *Nature Reviews. Drug Discovery, 3*, 1023–1035.

Doi, Y., Kitamura, S., & Abe, H. (1995). Microbial synthesis and characterization of poly(3-hydroxybutyrate-co-3-hydroxyhexanoate). *Macromolecules, 28*, 4822–4828.

Dong, T., Kai, W., & Inoue, Y. (2007b). Regulation of polymorphic behavior of poly(butylene adipate) upon complexation with α-cyclodextrin. *Macromolecules, 40*, 8285–8290.

Dong, T., Kai, W., Pan, P., Cao, A., & Inoue, Y. (2007a). Effects of host-guest stoichiometry of α-cyclodextrin-aliphatic polyester inclusion complexes and molecular weight of guest polymer on the crystallization behavior of aliphatic polyesters. *Macromolecules, 40*, 7244–7251.

Dong, T., Mori, T., Pan, P., Kai, W., Zhu, B., & Inoue, Y. (2009). Crystallization behavior and mechanical properties of poly(ε-caprolactone)/cyclodextrin biodegradable composites. *Journal of Applied Polymer Science, 112*, 2351–2357.

Feng, L., Watanabe, T., He, Y., Wang, Y., Kichise, T., Fukuchi, T., et al. (2003). Phase behavior and thermal properties for binary blends of bacterial poly(3-hydroxybutyrate-co-3-hydroxyhexanoate)s with narrow-comonomer-unit compositional distribution. *Macromolecular Bioscience, 3*, 310–319.

Feng, L., Yoshie, N., Asakawa, N., & Inoue, Y. (2004). Comonomer-unit compositions, physical properties and biodegradability of bacterial copolyhydroxyalkanoates. *Macromolecular Bioscience, 4*, 186–198.

Harada, A., & Kamach, M. (1990). Complex formation between poly(ethylene glycol) and α-cyclodextrin. *Macromolecules, 23*, 2821–2823.

He, Y., & Inoue, Y. (2003). A-cyclodextrin-enhanced crystallization of poly(3-hydroxybutyrate). *Biomacromolecules, 4*, 1865–1867.

He, Y., Zhu, B., & Inoue, Y. (2004). Hydrogen bonds in polymer blends. *Progress in Polymer Science, 29*, 1021–1051.

Huang, F., & Gibson, H. W. (2005). Polypseudorotaxanes and polyrotaxanes. *Progress in Polymer Science, 30*, 982–1018.

Iwata, T., Doi, Y., Kasuya, K., & Inoue, Y. (1997). Visualization of enzymatic degradation of poly[(R)-3-hydroxybutyrate] single crystals by an extracellular PHB depolymerase. *Macromolecules, 30*, 833–839.

Li, J., Yang, C., Li, H., Wang, X., Goh, S. H., Ding, J. L., et al. (2006). Cationic supramolecules composed of multiple oligoethylenimine-grafted β-cyclodextrins threaded on a polymer chain for efficient gene delivery. *Advanced Materials, 18*, 2969–2974.

Loethen, S., Kim, J., & Thompson, D. H. (2007). Biomedical applications of cyclodextrin based polyrotaxanes. *Polymer Reviews, 47*, 383–418.

Luo, R. C., Xu, K. T., & Chen, G. Q. (2008). Effects of L-phenylalanine as a nucleation agent on the non-isothermal crystallization, melting behavior, and mechanical properties of poly(3-hydroxybutyrate-co-3-hydroxyhexanoate). *Journal of Applied Polymer Science, 110*, 2950–2956.

Misra, S. K., Valappil, S. P., Roy, I., & Boccaccini, A. R. (2006). Polyhydroxyalkanoate (PHA)/inorganic phase composites for tissue engineering applications. *Biomacromolecules, 7*, 2249–2258.

Mori, T., Dong, T., Yazawa, K., & Inoue, Y. (2007). Preparation of highly transparent and thermally stable films of α-cyclodextrin/polymer inclusion complexes. *Macromolecular Rapid Communications, 28*, 2095.

Okumura, Y., & Ito, K. (2001). The polyrotaxane gel: A topological gel by figure-of-eight cross-links. *Advanced Materials, 13*, 485–487.

Ooya, T., & Yui, N. (1999). Synthesis of theophylline–polyrotaxane conjugates and their drug release via supramolecular dissociation. *Journal of Controlled Release, 58*, 251–269.

Organ, S. J., & Barham, P. J. (1991). Nucleation, growth and morphology of poly(hydroxybutyrate) and its copolymers. *Journal of Materials Science, 26*, 1368–1374.

Pan, P., Liang, Z., Nakamura, N., Miyagawa, T., & Inoue, Y. (2009). Uracil as nucleating agent for bacterial poly[(3-hydroxybutyrate)-co-(3-hydroxyhexanoate)] copolymers. *Macromolecular Bioscience, 9*, 585–595.

Peet, J., Rusa, C. C., Hunt, M. A., Tonelli, A. E., & Balik, C. M. (2005). Solid-state complexation of poly(ethylene glycol) with α-cyclodextrin. *Macromolecules, 38*, 537–541.

Rusa, C. C., Wei, M., Bullions, T. A., Rusa, M., Gomez, M. A., Porbeni, F. E., et al. (2004). Controlling the polymorphic behaviors of semicrystalline polymers with cyclodextrins. *Crystal Growth & Design, 4*, 1431–1441.

Sato, H., Nakamura, M., Padermshoke, A., Yamaguchi, H., Terauchi, H., Ekgasit, S., et al. (2004). Thermal behavior and molecular interaction of poly(3-hydroxybutyrate-co-3-hydroxyhexanoate) studied by wide-Angle X-ray diffraction. *Macromolecules, 37*, 3763.

Shuai, X., Porbeni, F. E., Wei, M., Bullions, T., & Tonelli, A. E. (2002). Inclusion complex formation between α,γ-cyclodextrins and a triblock copolymer and the cyclodextrin-type-dependent microphase structures of their coalesced samples. *Macromolecules, 35*, 2401–2405.

Sudesh, K., Abe, H., & Doi, Y. (2000). Synthesis, structure and properties of polyhydroxyalkanoates: biological polyesters. *Progress in Polymer Science, 25*, 1503–1555.

Szejtli, J. (1998). Introduction and general overview of cyclodextrin chemistry. *Chemical Reviews, 98*, 1743–1754.

Tajima, K., Dong, T., Hirose, K., Aoyama, T., & Inoue, Y. (2008). Inducing rapid crystallization of slowly-crystallizable copolyester by in situ generation of crystalline nuclei in melt of copolyester. *Polymer Journal, 40*, 300–301.

Takeo, K., & Kuge, T. (1970). Complexes of starchy materials with organic compounds. *Agricultural and Biological Chemistry, 34*, 1787–1794.

Verhoogt, H., Ramsay, B. A., & Favis, B. D. (1994). Polymer blends containing poly(3-hydroxyalkanoate)s. *Polymer, 35*, 5155–5169.

Wei, M., Davis, W., Urban, B., Song, Y., Porbeni, F. E., Wang, X., et al. (2002). Manipulation of nylon-6 crystal structures with its α-cyclodextrin inclusion complex. *Macromolecules, 35*, 8039–8044.

Wei, M., Shuai, X., & Tonelli, A. E. (2003). Melting and crystallization behaviors of biodegradable polymers enzymatically coalesced from their cyclodextrin inclusion complexes. *Biomacromolecules, 4*, 783–792.

Wenz, G. (1994). Cyclodextrins as building blocks for supramolecular structures and functional units. *Angewandte Chemie International Edition, 33*, 803–822.

Wenz, G., Han, B., & Müller, A. (2006). Cyclodextrin rotaxanes and polyrotaxanes. *Chemical Reviews, 106*, 782–817.